

# Controller design issues in the feedback control of radio frequency plasma processing reactors

Shahid Rauf<sup>a)</sup> and Mark J. Kushner<sup>b)</sup>

*Department of Electrical and Computer Engineering, University of Illinois, Urbana, Illinois 61801*

(Received 9 December 1998; accepted 19 February 1999)

Feedback control has the potential for improving the reliability and performance of radio frequency (rf) plasma processing reactors for microelectronics etching, deposition, and cleaning applications. Implementation of real-time-control strategies has been slowed by lack of analytic or computational tools to design or optimize systems. To address this need, the virtual plasma equipment model (VPEM) has recently been developed for investigating issues related to feedback control in rf plasma processing equipment. The VPEM has been employed to investigate feedback control of inductively coupled plasma processing reactors for polysilicon etching and, in this article, results from these studies are used in a discussion of controller design, control strategies, and validation of the VPEM. It is demonstrated that response surface based controllers best operate in combination with corrections from an unstructured controller such as a proportional-integral derivative, which relaxes the inherent rigidity of the model-based controller. Since the behavior of plasma processing reactors generally changes over time due to, for example, coatings of the walls, it was found advantageous to make the controllers adaptive. © 1999 American Vacuum Society. [S0734-2101(99)05003-4]

## I. INTRODUCTION

The reliability of modern industrial processes and advanced engineering products is in large part due to the use of feedback control. In recent years, the microelectronics manufacturing community has shown considerable interest in incorporating feedback control in plasma processing equipment to improve their reliability, yield, and performance.<sup>1</sup> Although even basic control techniques can improve performance, the success of feedback control ultimately depends on the optimal choice of sensors, actuators, and control strategy. This procedure is fairly involved in plasma aided manufacturing tools for microelectronics fabrication because the quantities of interest (e.g., etch or deposition rate, etch uniformity) are often difficult to directly measure. As a result, one usually relies on indirect control of quantities that are more easily measured and which correlate to the process parameters to be controlled. Acknowledging that plasma processing is complex and often not well characterized, statistical techniques are often used in which sensor data is monitored and the process is automatically or manually tuned in response to error signals.<sup>2,3</sup> On the other hand, it has also been demonstrated that controllers based on reduced order models can be successfully used for feedback control of plasma processing reactors.<sup>4</sup> There are many control strategies that lie in between these two extremes. For example, control techniques using response surfaces are based on empirical models which are developed experimentally or computationally, and relate the actuators settings to sensor data.<sup>3,5,6</sup> The success of these techniques depends on how

well the quantities controlled by the actuators are correlated to the sensors, and the degree of robustness of the controllers. Proportional-integral-derivative (PID) controllers,<sup>7,8</sup> controllers based on neural networks<sup>9</sup> and dynamic controllers based on system identification techniques<sup>10</sup> have also been used in plasma processing related studies with the goals of increasing these correlations and improving robustness.

To aid in evaluation of control strategies, we recently developed a computational tool called the virtual plasma equipment model (VPEM),<sup>6</sup> which consists of a plasma equipment model coupled to actuator, sensor, and controller modules. The sensor module emulates the output of experimental sensors (e.g., optical and electrical measurements). The controller module is programmable and uses the output of the sensor module to recommend changes in process variables. The actuator module then changes process parameters (e.g., power, pressure, and voltage) in the plasma equipment model. Using the VPEM, response surface based controllers have been investigated to compensate for external disturbances and nullify the effect of long term drifts in chamber conditions. In this article, we extend the previous work and address additional issues related to validation of the VPEM, improvement of controller design, and control strategies for polysilicon etching. The VPEM makes use of the hybrid plasma equipment model (HPEM)<sup>11-13</sup> for simulating the plasma reactor. The HPEM has been validated against experiments for many different plasma systems and gases,<sup>11,13-15</sup> and so we address experimental validation of the control aspects of the VPEM in this article. The example cases address control of an inductively coupled plasma (ICP) in Cl<sub>2</sub> for polysilicon etching using sensors for Cl\* emission from the bulk plasma and ion flux at the substrate (which can be measured using electrical sensors<sup>16,17</sup>).

The modeling platform is discussed in Sec. II followed by

<sup>a)</sup>Present address: Motorola, Predictive Engineering Lab, 3501 Ed Bluestein Blvd., Austin, TX 78721; electronic mail: ra8952@email.sps.mot.com

<sup>b)</sup>Author to whom correspondence should be addressed; electronic mail: mjk@uiuc.edu

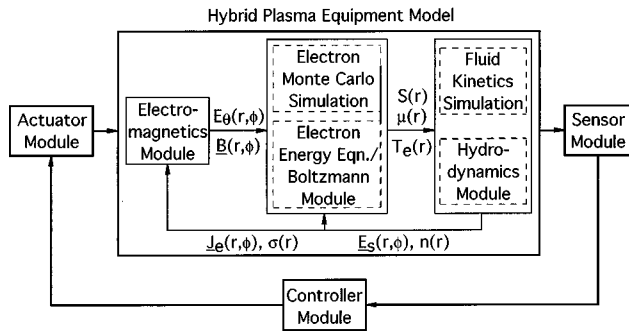


FIG. 1. Schematic of the virtual plasma equipment model (VPEM).

a summary of validation of the VPEM in Sec. III. Controller design issues related to feedback control of ICPs in  $\text{Cl}_2$  for polysilicon etching are discussed in Sec. IV. Section V contains our concluding remarks.

## II. DESCRIPTION OF THE MODEL

The computational tool we used in this investigation, the virtual plasma equipment model (VPEM), has been previously described in detail,<sup>6</sup> so it is only briefly discussed here. The VPEM is an extension of the hybrid plasma equipment model (HPEM),<sup>11–13</sup> a comprehensive plasma equipment simulation tool. In the VPEM, the HPEM is treated as a virtual plasma processing reactor that is linked to sensor, actuator, and programmable controller modules. (See Fig. 1.) The sensor module emulates measurements of experimental sensors. The sensors (and their experimental analogues) include spatially averaged densities of plasma species (optical emission spectroscopy), ion flux to surfaces (electrical measurements), ion energy flux to surfaces (ion energy analyzer), species flux at the pump port or other locations on the walls (residual gas analyzer), and plasma density (Langmuir probe or microwave interferometry). The sensor data is passed to the controller module which estimates changes in actuator settings required to bring sensor signals to a desired set point. Following commands from the controller module, the actuator module adjusts quantities in the HPEM that correspond to actuators such as gas pressure, inductively coupled power, capacitively coupled power, applied voltage on electrodes, gas flow rate, and mole fraction of gases in the feed. The HPEM is then executed using the updated actuator settings.

## III. VALIDATION OF THE VPEM

To validate the control aspects of the VPEM, feedback control experiments<sup>7</sup> in a magnetized inductively coupled plasma (ICP) reactor<sup>18</sup> were simulated. In these experiments, Sarfaty *et al.* implemented a two-color laser interferometer to measure the etch rate of polysilicon in a chlorine plasma in real time. After determining that the etch rate is well correlated with the rf bias power, the etch rate was controlled using rf bias power as the actuator. Both PID and model-based controllers were implemented and it was determined

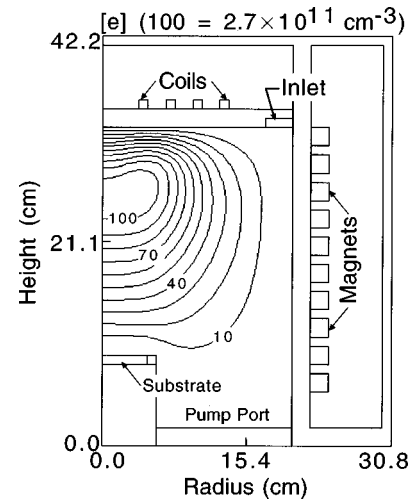


FIG. 2. Electron density in the magnetized ICP reactor for 1000 W inductive power deposition,  $\text{Cl}_2/\text{Ar}=96/4$  at 4 mTorr, 30 sccm gas flow, 100 V rf bias at 13.56 MHz. The contour labels indicate the percentage of the maximum value noted at the top of the figure.

that corrections from model-based controllers can significantly improve the response time and accuracy of the PID controller.

In applying the VPEM to this problem, etch rate was used as the sensor, and was computed using Dane and Mantei's semiempirical relationship for polysilicon etch rates in chlorine plasmas.<sup>19</sup> The etch rate  $ER$  ( $\text{\AA min}^{-1}$ ) is

$$ER = \left( \frac{1}{2300P^{0.5}} + \frac{1}{23(J_i V_s - 85)} \right)^{-1}, \quad (1)$$

where  $P$  is the gas pressure in mTorr and  $J_i V_s$  is the ion power flux to the substrate in  $\text{mW cm}^{-2}$ . In the VPEM, the ion current density  $J_i$  was obtained from the ion fluxes to the wafer.  $V_s$ , the sheath potential, was approximated as the difference between the time averaged electrode voltage and plasma potential in the presheath.

In the low pressure, high plasma density, inductively coupled systems of interest, the magnitude of the ion current entering the sheath is largely determined by the inductively coupled power.<sup>11</sup> Since the sheath is at best only a few hundred microns thick, the addition of an rf bias voltage to the substrate produces little additional plasma heating. The bias voltage therefore does not significantly increase the plasma density or ion current into the sheath, but does accelerate ions into the substrate. Since the bias power is  $J_i V_s$ , if the inductively coupled power is held constant so that the ion current entering the sheath is nearly constant, bias power can be controlled by varying the bias voltage. The rf bias voltage on the substrate was therefore used as the actuator.

The reactor geometry used in the model is shown in Fig. 2 along with the electron density for a gas mixture of  $\text{Cl}_2/\text{Ar}=96/4$  at 4 mTorr, gas flow of 30 sccm, 1000 W inductively coupled power, and 100 V rf bias (13.56 MHz) applied to the substrate. Gas is injected into the reactor through a ring nozzle at the top of the chamber and is exhausted through a pump port at the bottom of the reactor. A

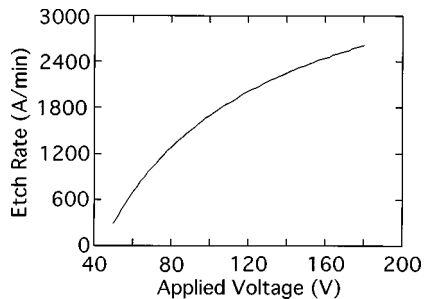


FIG. 3. Polysilicon etch rate as a function of applied rf voltage amplitude in the magnetized ICP reactor for 1000 W inductive power deposition,  $\text{Cl}_2/\text{Ar}=96/4$  at 4 mTorr and 30 sccm gas flow.

silicon wafer with a polysilicon coating is placed on the substrate. The volume of the reactor below the substrate was truncated in the calculation because it does not appreciably affect the plasma characteristics. In the experimental reactor, the field lines of the cusps of the magnetic bucket are predominantly in the horizontal plane ( $r-\phi$  in azimuthal geometry). Since these field lines cannot be resolved in our azimuthally symmetric two-dimensional simulation, the magnetic dipoles were oriented so that the cusps of the magnetic field were in the  $r-z$  plane. The consequences of both magnetic field configurations is to improve electron confinement in the radial direction.

The computed polysilicon etch rate is shown in Fig. 3 as a function of the applied voltage for the conditions of Fig. 2. At low voltages, the etching process is in the ion energy-starved regime where the neutral reactants are plentiful. The etch rate therefore increases almost linearly as a function of the bias voltage. Above 80 V, the etch process gradually shifts to the neutral-starved regime where the etch process is limited by the availability of Cl atoms and etch rate flattens out.

We first consider the problem in which a PID controller is used to dynamically adjust the etch rate so that it follows a prescribed time dependence. Results from the simulation are compared with the corresponding experimental results<sup>7</sup> in Fig. 4. The controller frequency, the rate at which the controller receives sensor data and issues commands to the actuators, is 10 Hz in the simulation. The simulation, in general, tracks the set point in the same manner as the experiment. Since the controller has no knowledge about the dynamic response of the system, each step change in the set point leads to large under-damped oscillations. It also takes the controller several seconds to respond to the step change in input command. The controller response changes from under to overdamped in the experiment after 200 s. This may be due to a change in plasma or reactor conditions, or it is an artifact of the low pass filter that is used to suppress noise. This effect is not captured in the simulation.

Sarfaty *et al.*<sup>7</sup> found that controller response could be considerably improved (made faster with less overshoot) by including corrections from a response surface based model. Results from this exercise are shown in Fig. 5. In the VPBM, corrections from the response surface were formulated in the

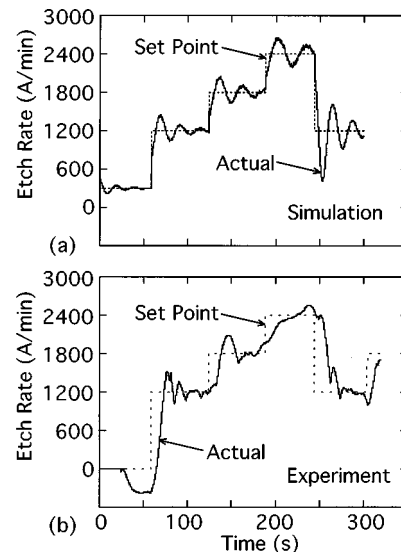


FIG. 4. Control of polysilicon etch rate in the magnetized ICP reactor using a PID controller. (a) Simulation results, (b) experimental results by Sarfaty *et al.*

following manner. A least mean square quadratic fit of etch rate as a function of rf bias voltage  $V_M$  was performed,

$$ER = c_0 + c_1 V_M + c_2 V_M^2, \quad (2)$$

where  $c_0$ ,  $c_1$ , and  $c_2$  are constants. After differentiating Eq. (2), we obtain

$$dV_M = d[ER] / (c_1 + 2V_M c_2), \quad (3)$$

where  $d[ER]$  and  $dV_M$  are small changes in the etch rate and applied voltage recommended by the model. The change in actuator settings  $\Delta V$  was determined using,

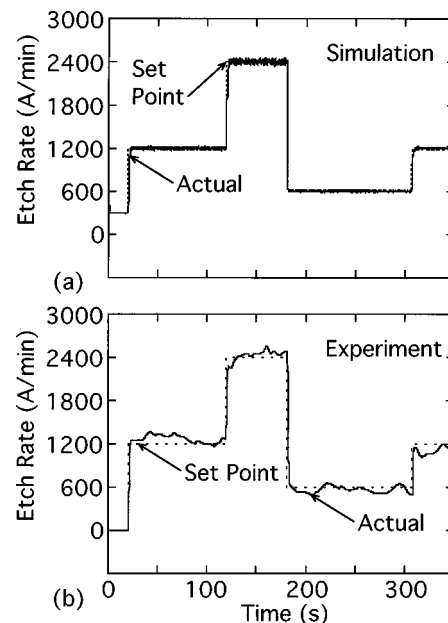


FIG. 5. Control of polysilicon etch rate in the magnetized ICP reactor using a PID controller with contribution from a response surface based model. (a) Simulation results, (b) experimental results by Sarfaty *et al.*

$$\Delta V = FF \cdot dV_M + (1 - FF) \cdot dV_{PID}, \quad (4)$$

where  $FF$  is the feed-forward ratio and  $dV_{PID}$  is the change in rf bias voltage recommended by the PID controller. Results from the experiments and simulation are shown in Fig. 5 for  $FF=0.25$ . 5% random noise has been added to the output of the sensor and a three-step exponentially weighed low pass filter was connected in series with the controller. Corrections from the model-based controller have made the controller response faster and the overshoot has been eliminated. It was found that very little feed forward contribution is needed for the sensor to closely track the set point. In the above results, deviations from the set point were only significant when  $FF$  was less than 0.05. Comparisons of computational results with experiments have shown that the real time control algorithms used in the VPDM are valid as long as the controller time step is larger than the time required for plasma conditions to settle down to quasisteady state after a step change in actuators. For the sensor and actuator considered here, this time is estimated to be less than 0.1 s.

#### IV. CONTROLLER DESIGN ISSUES

Response surface based controllers are generally effective in compensating for actuator drifts and controlling well-structured processes. In this section, we examine the behavior of response-surface based controllers studied earlier<sup>6</sup> in situations where their performance is less than adequate and we suggest strategies to improve the controller performance. Noise and uncertainties are always present in real systems and they can deteriorate the controller performance. Other components (e.g., low pass filter to suppress noise) may also be connected in series with the controller and which change the response of the controller.

To investigate the consequences of noise and an exponentially weighed low pass filter on operation of the PID- $FF$  controller discussed in the previous section, we ran simulations where 5% random noise was added to the sensor output, a three-step exponentially weighed filter was connected before the controller and feed-forward ratio ( $FF$ ) was varied between 0 and 1. The results are shown in Figs. 6(a)–6(d). The reactor and operating conditions are the same as those in the previous section. When  $FF=0$ , the controller is a PID so there is significant delay in response after step changes in set point and, for this particular case, there is an overdamped response. As  $FF$  is increased to 0.25, the contribution from the model-based controller significantly reduces the response time and the controller is able to track the set point. When  $FF$  is increased further, we find that there is little gain in controller performance. In fact, there are reasonably large oscillations in etch rate when the set point changes, which results from the interaction of the model-based controller with the low pass filter. This interaction is demonstrated in Fig. 6(e) where the etch rates are shown without the low pass filter. Even though the noise level has increased because of the absence of the low pass filter, the large spikes after step changes in set point have been avoided. If the etch rate is large, the oscillations can take the system into parameter

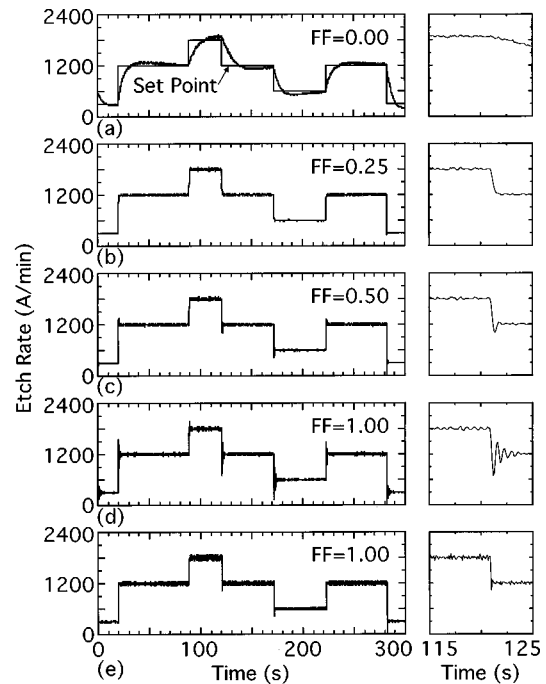


FIG. 6. Behavior of a PID controller with corrections from a model-based controller. Results in (a)–(d) are for different values of  $FF$ . The low pass filter is not used in (e). The right panels contain enlarged results for 115–125 s.

spaces where the response surface based model is no longer valid and the system can become unstable. These results suggest that use of a stand-alone model-based controller is not the best option in situations where noise is present or interaction with other systems, such as the filter, may occur because of the model-based controller's inherent rigidity. In those cases, using contributions from an unstructured controller as a PID will make the system more stable without deteriorating performance.

The controller-filter interaction occurs because the model based controller was designed for a specific sensor-actuator relationship. That is, when the control changes an actuator setting to modify a process parameter, it “expects” a predictable response. By adding the low pass filter the response of the system (which now consists of the plasma processing reactor and filter in series) to changes in actuator settings is different than that used for the design of the controller. As a result, the controller is no longer able to correctly specify changes actuator settings when sensor signals change. Since the low pass filter will, by its nature, always change the system response, controller-filter interactions can be expected to be strong for most common filter topologies. One way to avoid this problem is to design the controller with the low pass filter in place, as might be accomplished by treating the filter as a component of the reactor.

The next series of investigations use the ICP reactor shown in Fig. 7(a). The reactor has a four-turn antenna coil on top of a dielectric window. Gas is injected through a showerhead and is exhausted at the bottom of the chamber. A chlorine chemistry will be used to etch a poly-Si wafer. The electron density and electron source function are shown

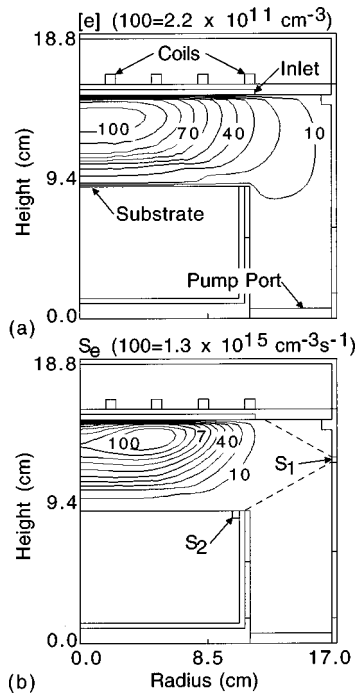


FIG. 7. Plasma properties for an ICP reactor ( $\text{Ar}/\text{Cl}_2=70/30$ , 20 mTorr, 500 W). (a) Electron density, (b) electron source function. The sensor for  $\text{Cl}^*$  emission is located at  $S_1$  and ion flux is measured at  $S_2$ . The contour labels indicate the percentage of the maximum value noted at the top of the figure.

in Fig. 7 for an  $\text{Ar}/\text{Cl}_2=70/30$  gas mixture at 20 mTorr and 500 W inductive power deposition. The electrons are predominantly being produced in a toroidal region below the coils [see Fig. 7(b)]. They are, however, able to diffuse out of the region of production and the peak electron density occurs on axis.

The polysilicon etch rate in a  $\text{Cl}_2$  plasma is a function of the ion flux, ion energy, and neutral  $\text{Cl}$  flux to the substrate, and so the etch rate can be regulated by controlling these factors. The two sensors used for this purpose measure the emission from  $\text{Cl}^*$  within the observation cone shown in Fig. 7(b), and ion flux at the sensor  $S_2$ .  $\text{Cl}^*$  is produced through electron impact excitation of  $\text{Cl}$  and its emission is an indication of  $\text{Cl}$  flux to the substrate. Ion flux can be measured using electrical sensors<sup>16</sup> at off-axis locations and should be indicative of ion flux to the wafer. If the sheath is collisionless, the ion energy can be estimated from the sheath potential and can be controlled using the rf bias voltage. In these experiments, the bias voltage is however kept constant, so power flux to the substrate is dominantly controlled by ion flux. The sensor signals are controlled using inductively coupled power and gas pressure as actuators. As in Ref. 6, the controllers are designed using response surface based models. The response surfaces showing the dependence of  $\text{Cl}^*$  density and total ion flux at  $S_2$  on the actuators are plotted in Fig. 8. An increase in inductively coupled power leads to nearly linear increases in both  $\text{Cl}^*$  emission and ion flux to the sensor.  $\text{Cl}^*$  emission, converted to number density here, increases with pressure as  $\text{Cl}_2$  is largely dissociated at these powers. An increase in pressure decreases ion flux to

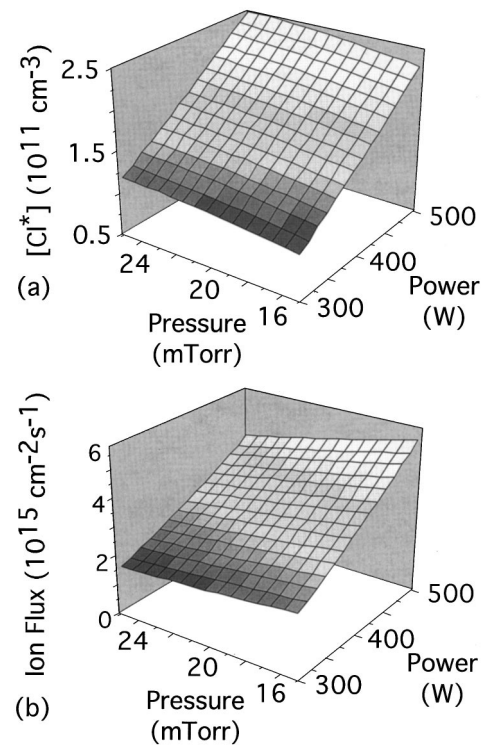


FIG. 8. Response surfaces for design of controllers for the reactor shown in Fig. 8. (a)  $\text{Cl}^*$  density and (b) ion flux to the sensor  $S_2$  as a function of gas pressure and inductive power deposition.

the wafer because the plasma becomes more collisional and the mean ion velocity decreases.

Using the response surfaces shown in Fig. 8 and the controller design technique described in Ref. 6, controllers were employed to maintain sensor signals at specified values. The basic operation of this controller is shown in Fig. 9. For these results, the gas pressure was initially 20 mTorr and inductive power deposition was 400 W. The actuators were kept constant until  $T=5$ , at which point the inductive power is increased by 5%. This increases both  $\text{Cl}^*$  density and ion flux. In response to these changes in sensor signals, the controller adjusted the actuators so that the sensor signals returned to their original values. In the first time step, the controller decreased both pressure and power. In the second time step, the controller recouped the decrease in pressure. Since the response surfaces provide an accurate representation of the perturbed system, the controller is able to restore the system to its initial state in only a few time steps.

We next investigated the behavior of the model-based controller in response to a change in gas composition at the inlet. The results are shown in Fig. 10. The inductive power deposition was initially 400 W, gas pressure is 20 mTorr, and gas mixture is  $\text{Ar}/\text{Cl}_2=70/30$ . At  $T=5$ , the input  $\text{Cl}_2$  mole fraction was increased to 36%. An increase in  $\text{Cl}_2$  results in more  $\text{Cl}$  production and consequently an increase in  $\text{Cl}^*$  density. However, electron loss through dissociative attachment to  $\text{Cl}_2$  increases which results in smaller positive ion densities and a lower ion flux to the wafer. In response to these changes in the sensor signals, the controller decreases

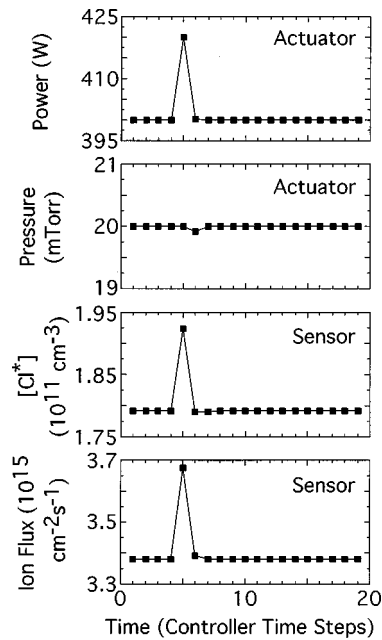


FIG. 9. Sensor and actuator time histories for the response-surface based controller compensating for a drift in inductive power deposition.

gas pressure and increases inductive power, the result of which is to dissociate more  $\text{Cl}_2$ . In a few time steps, the sensor signals return to their original values in spite of the fact that the controller is operating in a system that is differ-

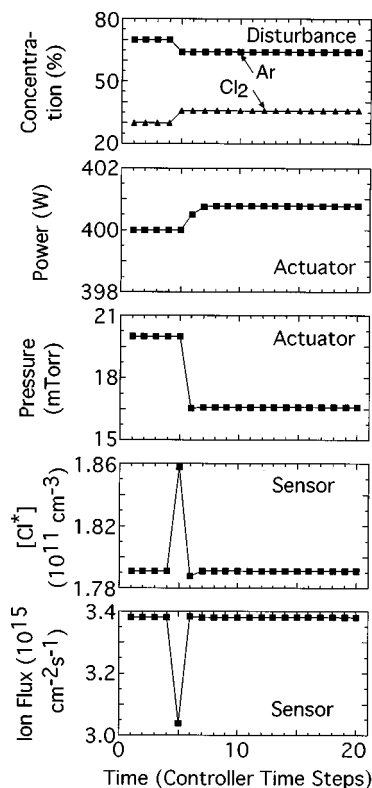


FIG. 10. Sensor and actuator time histories for the response-surface based controller compensating for a change in gas composition.

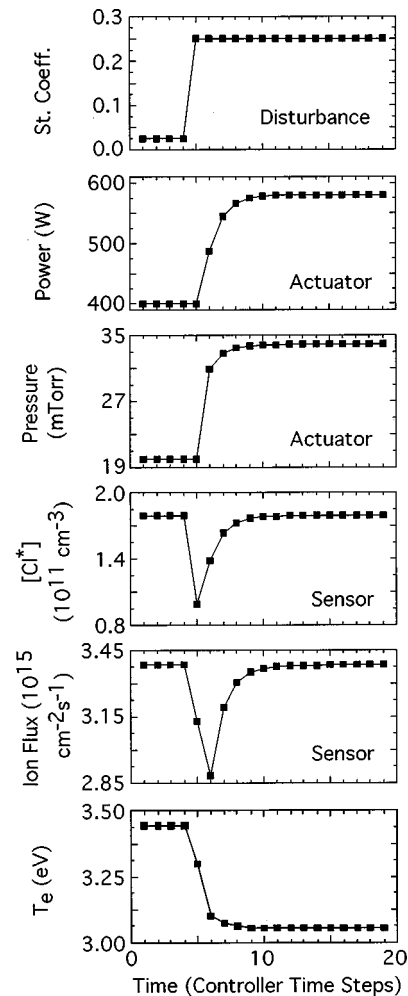


FIG. 11. Sensor, actuator, and electron temperature time histories for the response-surface based controller compensating for a change in sticking coefficient of  $\text{Cl} \rightarrow \text{Cl}_2$  at reactor walls.

ent ( $\text{Ar}/\text{Cl}_2=64/36$ ) than the one it was designed for ( $\text{Ar}/\text{Cl}_2=70/30$ ).

Plasma and reactor conditions generally evolve over time and controllers should perform adequately over the whole range of conditions that may be encountered. One factor that contributes to evolving reactor conditions is passivation and polymer buildup on reactor walls. This process takes place over a time period much longer than what is practically feasible to simulate. To investigate the operation of the model-based controller in response to long-term drifts, we instead changed the reactor conditions suddenly, in this case by artificially changing the sticking coefficient of  $\text{Cl} \rightarrow \text{Cl}_2$  at the walls. The results for this problem are shown in Fig. 11. Inductive power deposition was initially 400 W, gas pressure is 20 mTorr, and sticking coefficient is 0.025. At  $T=5$ , the sticking coefficient was increased to 0.25, which results in a decrease in  $\text{Cl}^*$  emission because more  $\text{Cl}$  atoms are converted to  $\text{Cl}_2$  at the walls and the larger  $\text{Cl}_2$  density decreases the electron density (and rate of electron impact excitation) due to dissociative attachment. The ion flux to the sensor also decreases because the increase in  $\text{Cl}_2$ , which reduces

the electron density, also produces a decrease in positive ion density. In response to these changes in sensor signals, the controller increases the power and the pressure to produce more electron impact dissociation and ionization until the sensors return to their original values.

It should be noted that, since the initial change in sensor signals was large and the system parameters of the perturbed reactor were quite different from those for which the controller was designed, many controller time steps were required for the sensors to return to their original values. Also, the ion flux initially drifted in the wrong direction, which indicates that the corrections to power and pressure first suggested by the response surface based model were incorrect.

Since controllers should be able to operate in widely varying conditions, the above results suggest that it is advisable to use adaptive controllers so that they can adjust to changes in the reactor and plasma conditions. The adaptive algorithm we used to demonstrate this advantage modifies the response surface based model so that it better reflects the present conditions. The controllers are based on a polynomial approximation of the response surfaces,

$$f_j(x, c) \equiv y_j = c_{0j} + \sum_{k=1}^n c_{1jk}(x_k - x_{k0}) + \sum_{k=1}^n \sum_{l=1}^n c_{2jkl}(x_k - x_{k0})(x_l - x_{l0}), \quad (5)$$

where  $y_j$  is the  $j$ th sensor output,  $x_k$  is the  $k$ th actuator setting,  $c_{0j}$ ,  $c_{1jk}$ , and  $c_{2jkl}$  are constant coefficients,  $n$  is the number of actuators and sensors,  $x$  is the set  $\{x_k: 1, 2, \dots, n\}$ , and  $c$  is the set of all constant coefficients. The goal of the adaptive algorithm is to adjust the constant coefficients so that Eq. (5) better represents the actuator-sensor relationship. This is accomplished using measurements  $(x', y'_j)$  that are randomly distributed about the operating point. These measurements can be made in real time or they can be obtained from an archive of previous measurements. The number of the measurements used for adapting the controller should be larger than the number of coefficients that are to be adjusted  $m$  (e.g.,  $m=6$  for  $n=2$ ). With these measurements, the following iterative procedure is used to adjust the coefficients:

- (1) Randomly make or select  $m$  measurements near the operating operating point from the sample set of such measurements.
- (2) Write the following equations in a matrix form and solve for  $c_{\text{req}}$ :
 
$$[y'_j]_k = [f_j(x', c_{\text{req}})]_k, \quad k = 1, 2, \dots, m. \quad (6)$$
- (3) Compute new values for the coefficients using
 
$$c_{\text{new}} = c_{\text{old}} + \alpha(c_{\text{req}} - c_{\text{old}}), \quad \text{where } \alpha \ll 1. \quad (7)$$
- (4) If  $|c_{\text{new}} - c_{\text{old}}|/c_{\text{old}} < \epsilon$  (where the maximum error  $\epsilon \ll 1$ ), stop iterating. Otherwise copy  $c_{\text{new}}$  to  $c_{\text{old}}$  and go to step 1.

The number of sample measurements should generally be reasonably larger than  $m$  so that the modified model is not strongly weighted towards any particular measurements. If  $\alpha$

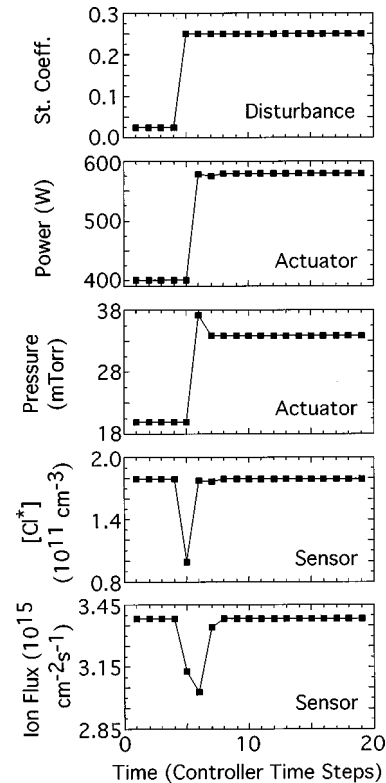


FIG. 12. Sensor and actuator time histories for the response-surface based controller compensating for a change in sticking coefficient of  $\text{Cl}(\rightarrow \text{Cl}_2)$  at reactor walls. The adaptive algorithm is used to retune the model after  $T = 5$ .

is close to 1, fewer iterations of the above procedure are required, but the values of the coefficients will fluctuate and the iterative scheme may diverge. Small values of  $\alpha$  will result in a large number of iterations but the solution would be more stable.

The adequacy of the above scheme was tested for the problem in which the  $\text{Cl}$  sticking coefficient at the wall was changed. The conditions were similar to those considered earlier for Fig. 11 and the results are shown in Fig. 12. The adaptive algorithm is implemented just after the sticking coefficient is changed ( $T=5$ ) to adjust the response surface based model. Comparing the results in Figs. 11 and 12, we find that, due to the adaptive adjustment, the controller response is faster and the overshoot of ion flux in the wrong direction is smaller. The controller with the adaptive feature, therefore, fares better when plasma or reactor conditions change.

The random measurements used for adaptive tuning of the controller should ideally span as much of the actuator parameter space as possible. If the measurements are all localized close to the operating point, the adaptive algorithm might not be able to accurately access the nonlinearities in the sensor-actuator relationship. This is demonstrated in Fig. 13 where we consider the same problem as in Fig. 12 but the random measurements are restricted to 20%, 50%, and 70% of the parameter space in Fig. 8. Since the dependence of  $\text{Cl}^*$  density on power and pressure is almost linear, the resulting

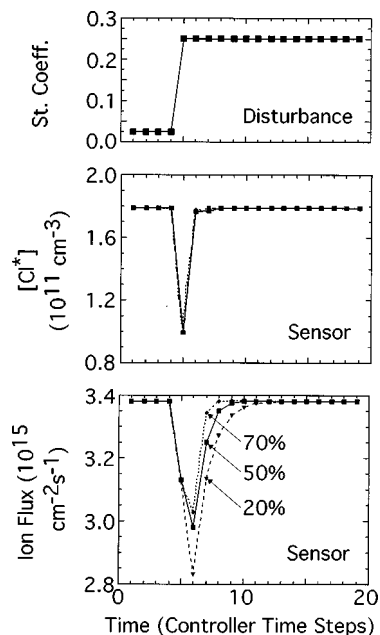


FIG. 13. Sensor time histories for the response-surface based controller compensating for a change in sticking coefficient of  $\text{Cl}(\rightarrow\text{Cl}_2)$  at reactor walls. The adaptive algorithm is used to retune the model after  $T=5$ . The range of random measurements used for adaptive tuning of controller is 20%, 50%, and 70% of the parameter space in Fig. 8.

sensor signals are not significantly effected by expanding the range of random measurements to capture the nonlinearities. However, the dependence of the ion flux on the actuator settings is slightly nonlinear [see Fig. 8(b)] and the performance of the adaptively tuned controller considerably improves as the range of random measurements is increased.

It is important to note that in the problems considered in Figs. 10–13, even though the sensor signals return to their unperturbed values, other quantities such as electron density and temperature may be different in the final steady state than before the perturbation. This is because the controller is not designed to regulate quantities other than the sensors and there may be many sets of reactor conditions which provide the desired sensor signals. This situation is illustrated in Fig. 11 where the time history of the electron temperature above the substrate is shown along with the sensor signals and actuator settings. Even though the sensor signals have been restored to their preperturbed values, the electron temperature is different in the initial and final states. Such a situation could be important in, for example, consideration of charging damage which depends on electron temperature.<sup>20</sup> Changes in ancillary plasma characteristics will, in general, occur if the perturbation is due to factors that are not built into the controller design. The controller can only bring the sensors back to their original settings and not necessarily bring the entire system to its original state.

## V. CONCLUDING REMARKS

Using a computational tool, the virtual plasma equipment model, feedback control of inductively coupled plasma processing reactors has been investigated. Some of the issues

addressed in this article include experimental validation of the VPDM, improvements in controller design, and control strategies for polysilicon etching in  $\text{Cl}_2$  based chemistries. Controllers that have built-in information about the sensor-actuator relationship, such as a response surface based controller, were found to be effective in compensating for actuator drifts or nullifying the effects of external perturbations. Response surface based controllers however best operate in combination with a contribution from an unstructured controller such as a PID, which relaxes the inherent rigidity of the model-based controller. This makes the controller more stable and robust against noise and other disturbances. Since the behavior of plasma processing equipment generally changes over time, an adaptive controller that periodically adjusts itself to changing plasma conditions was found to considerably improve performance.

There are many factors that one would ideally like to simultaneously control in, for example, a plasma process, such as rate, uniformity, and profile. Cause and effect relationships are however quite complicated in plasma processing reactors and any automatic control scheme that regulates a limited number of these factors will likely change parameters which are not being monitored. It was, for example, shown that although a response surface based controller adequately regulated the sensor signals of  $\text{Cl}^*$  emission and ion flux, the electron temperature changed during the process. Since multivariable controllers that are able to control all process parameters will not necessarily be practical, it is important when developing a control strategy to assess the consequences of actuator adjustments on noncontrolled process parameters that may impact the final product.

## ACKNOWLEDGMENTS

The authors would like to thank M. Sarfaty and N. Hershkowitz for useful discussions and supplying the experimental data, and P. Khargonekar for his advice. This work was supported by the Air Force Office of Scientific Research through the University of Michigan Multidisciplinary University Research Initiative, the Semiconductor Research Corp., and the University of Wisconsin Engineering Research Center for Plasma Aided Manufacturing.

<sup>1</sup>*Process Control, Diagnostics, and Modeling in Semiconductor Manufacturing*, edited by M. Meyyappan, D. Economou, and S. W. Butler (Electrochemical Society, New York, 1995), Vols. 1 and 2.

<sup>2</sup>C. J. Spanos, H. F. Guo, A. Miller, and J. Levine-Parrill, *IEEE Trans. Semicond. Manuf.* **5**, 308 (1992).

<sup>3</sup>P. K. Mozumder and G. G. Barna, *IEEE Trans. Semicond. Manuf.* **7**, 1 (1994).

<sup>4</sup>M. Chandok, P. D. Hanish, and J. W. Grizzle, in *Process Control, Diagnostics, and Modeling in Semiconductor Manufacturing*, edited by M. Meyyappan, D. Economou, and S. W. Butler (Electrochemical Society, New York, 1995).

<sup>5</sup>J. Stefani and S. W. Butler, *J. Electrochem. Soc.* **141**, 1387 (1994).

<sup>6</sup>S. Rauf and M. J. Kushner, *IEEE Trans. Semicond. Manuf.* **11**, 486 (1998).

<sup>7</sup>M. Sarfaty, C. Baum, M. Harper, N. Hershkowitz, and J. L. Shohet, in *Process Control, Diagnostics, and Modeling in Semiconductor Manufacturing*, edited by M. Meyyappan, D. Economou, and S. W. Butler (Electrochemical Society, New York, 1997).

- <sup>8</sup>P. L. G. Ventzek, N. Yamada, Y. Sakai, H. Tagashira, and K. Kitamori, *J. Vac. Sci. Technol. A* **13**, 2456 (1995).
- <sup>9</sup>E. A. Rietman, R. C. Frye, E. R. Lory, and T. R. Harry, *J. Vac. Sci. Technol. B* **11**, 1314 (1993).
- <sup>10</sup>B. A. Rashap *et al.*, *IEEE Trans. Semicond. Manuf.* **8**, 286 (1995).
- <sup>11</sup>M. J. Grapperhaus and M. J. Kushner, *J. Appl. Phys.* **81**, 569 (1997).
- <sup>12</sup>M. J. Grapperhaus, Z. Krivokapic, and M. J. Kushner, *J. Appl. Phys.* **83**, 35 (1998).
- <sup>13</sup>S. Rauf and M. J. Kushner, *J. Appl. Phys.* **83**, 5087 (1998).
- <sup>14</sup>S. Rauf and M. J. Kushner, *J. Appl. Phys.* **82**, 2805 (1998).
- <sup>15</sup>W. Z. Collison, T. Q. Li, and M. S. Barnes, *J. Vac. Sci. Technol. A* **16**, 100 (1998).
- <sup>16</sup>M. A. Sobolewski, *Appl. Phys. Lett.* **72**, 1146 (1998).
- <sup>17</sup>S. Rauf and M. J. Kushner, *Appl. Phys. Lett.* **73**, 2730 (1998).
- <sup>18</sup>C. Lai, R. Brunmeier, and R. C. Woods, *J. Vac. Sci. Technol. A* **13**, 2086 (1995).
- <sup>19</sup>D. Dane and T. D. Mantei, *Appl. Phys. Lett.* **65**, 478 (1994).
- <sup>20</sup>G. S. Hwang and K. P. Giapis, *Phys. Rev. Lett.* **79**, 845 (1997).